Figure Legends for Supplemental Figures

Supplemental Figure S1. CapD Hydrolysis Transition State Modeling. The gamma-linked poly-D-glutamate hydrolysis transition state model was generated and modeled as described in the Experimental Procedures. Briefly, the Rosetta Modeling Suite was used to minimize the protein-ligand interface energy given the distance (d_x : in angstroms) and angle (a_x : in degrees) constraints.

Supplemental Figure S2. Mass Spectrometry Analysis of CP. The purified CP protein was analyzed using electrospray liquid-chromatography tandem mass spectrometry (LCMS) on a TSQ Quantum Access. The expected weight of CP without the N-terminal methionine is 55285 Da, and with methionine is 55417 Da. The data for CP shows that the only major protein peak in the sample corresponds to the CP without the N-terminal methionine. The difference of 10 Da is well within the 0.02% error expected from the deconvolution of the liquid-chromatography electrospray ionization mass spectrometry charge envelope. The instrument was calibrated using the manufacturer recommended polytyrosine standard and the deconvolution was done using the manufacture provided ProMass Deconvolution 2.5 Software.

Supplemental Figure S3. Substrate versus Velocity Curves. The rate observed for CapD (**A**), CP (**B**), and F24H (**C**) was measured using three independent measurements for each enzyme as described in the Experimental Procedures section. Transpeptidation was measured as the observed activity in the presence of 5mM L-Glutamate and hydrolysis was measured as the observed activity in the absence of any exogenously added amino acids. The transpeptidation reaction for all three enzymes exhibited traditional Michaelis-Menten kinetics and was fit to (1), while the hydrolysis reaction was better fit to a substrate inhibition model (2).

Supplemental Figure S4. Purified CapD used for Determination of Kinetic Constants. The sample of CapD (right) used for determination of kinetic constants is to have more than 85% of the protein having undergone autocatalytic processing to active, dimeric protein. The Precision Plus Protein Kaleidoscope Standards (Bio-Rad, Hercules, CA) are labeled with molecular weights on the left in kDa.

Supplemental Figure S5. Far-UV and Melting Curve Circular Dichroism on CapD and CP. CD experiments were conducted as described in Experimental Procedures. (A) Far-UV CD spectra yielded similar ellipticity curves for CapD and CP, showing minimal difference between protein structures. (B) Melting curves display midpoint melting temperatures of 48.4^{o}C for CapD and 51.1^{o}C for CP, a 2.7^{o}C shift in favor of CP. For both experiments, four curves were accumulated and averaged without smoothing.

Supplemental Figure S6. Initial Screen of the Eighty-Four Computationally Designed Enzymes. Each protein variant was generated, expressed, purified, and assayed once as described in Experimental Methods. For each protein, the measured specific activity for transpeptidation and hydrolysis was normalized to the original activity measured for CP (Yellow, normalized at 1,1). Points below the line represent successful designs in which transpeptidation was more significantly decreased than hydrolysis. In particular the mutant F24H (red) is highlighted since it had a minimal effect on hydrolysis, but significantly decreased the transpeptidation reaction.

Supplemental Figure S7. Transpeptidation versus Hydrolysis Mechanism. CapD undergoes two half reactions. In the first half of the reaction, an acyl-enzyme is formed with the C-terminal fragment of the peptide substrate, and the N-terminal half is released. In the second half, a transpeptidation reaction can occur, in which an amine can act as an acceptor to the C-terminal fragment of the original peptide that is stuck on the enzyme, resulting in the formation of free enzyme and a new peptide. Alternatively, water can catalyze the hydrolysis of the acyl-enzyme resulting in the release of the C-terminal fragment as a free acid as well as the regeneration of free enzyme.

Supplemental Figure S8. Serum Dependence of Synthetic PDGA Cleavage. Each enzyme was incubated at several different concentrations of mouse serum, as indicated in the Figure. The relative rate of PDGA cleavage was measured and plotted as a function of serum concentration. Each measurement at each concentration was done once and therefore no error bars are included.

Substrate (μM)	1.000	0.500	0.250	0.125	0.063	0.031	0.016	0.008	0.004	0.002	0.001	0.000
Slope of Product Standard Curve (RFU x μM^{-1} x cm^{-1})	5032	4985	4992	4987	4852	4787	4806	4745	4708	4756	4616	4575

Supplemental Table S1. Fluorescence Intensity Calibration Curves. The conversion between relative fluorescence units (RFU) and product concentration was done by measuring the fluorescence intensity of a serially diluted product standard at each substrate concentration used in the Michaelis-Menten profiles. The slope of each curve reported was linear and had an R^2 value of greater than 0.99.

Amino Acid	capD	CP	F24H
Alanine	10.59 ± 0.39	12.62 ± 0.64	1.09 ± 0.02
Arginine	9.1 ± 0.28	12.88 ± 0.04	1.03 ± 0.02
Asparagine	12.53 ± 0.52	15.07 ± 0.31	1.04 ± 0.01
Aspartic Acid	2.61 ± 0.01	3.15 ± 0.29	-0.03 ± 0.13
Cysteine	11.28 ± 0.02	15.7 ± 0.26	0.81 ± 0.12
Glutamic Acid	10.76 ± 0.16	17.63 ± 0.12	0.51 ± 0.07
Glutamine	11.66 ± 1.86	16.9 ± 1.07	1.19 ± 0.06
Glycine	4.89 ± 1.20	6.56 ± 0.21	0.59 ± 0.03
Histidine	8.46 ± 0.96	12.28 ± 0.15	0.68 ± 0.13
Isoleucine	11.73 ± 0.47	14.95 ± 0.50	1.02 ± 0.11
Leucine	2.52 ± 0.04	3.82 ± 0.17	0.86 ± 0.06
Lysine	6.44 ± 0.08	7.73 ± 0.14	0.80 ± 0.03
Methionine	8.95 ± 0.04	12.89 ± 0.07	0.57 ± 0.02
Phenylalanine	10.03 ± 0.35	13.98 ± 0.09	0.89 ± 0.09
Proline	0.16 ± 0.02	1.57 ± 0.10	0.02 ± 0.03
Serine	12.32 ± 0.07	16.43 ± 0.14	1.09 ± 0.03
Threonine	8.51 ± 0.37	8.09 ± 1.42	0.82 ± 0.07
Tryptophan	1.54 ± 0.11	2.81 ± 0.09	-0.18 ± 0.04
Tyrosine*	4.51 ± 1.01	7.38 ± 0.03	0.38 ± 0.10
Valine	3.57 ± 0.36	4.87 ± 0.06	0.79± 0.09
Hydrolysis	0.66 ± 0.02	1.41 ± 0.01	0.56 ± 0.02

Supplemental Table S2. Amino Acid Specificity of CapD, CP, and F24H. The specific activity for each enzyme, CP, CapD, and F24H, was determined using 5mM of the amino acid acceptor, as described in Experimental Procedures. The specific activity for Tyrosine (Tyrosine*) was done at 1.8mM amino acid due to the limited solubility of tyrosine. Each activity was measured in triplicate with the errors representing the calculated standard deviation.

Supplemental Table S3. Observed hydrolysis and transpeptidation rates from the experimental screen of the computationally designed enzyme library. Each protein variant was generated, expressed, purified, and assayed as described in Experimental Methods. For each protein, the measured specific activity for transpeptidation and hydrolysis was normalized to the original activity measured for CP. As this was only an initial screen to identify potentially interesting protein variants from the designed library the expression and activity measurements for each member of the library was only done once.

Mutant Name (CP Numbering)	Relative Transpeptidation	Relative Hydrolysis
CP	1.0	1.0
CapD	0.5	0.7
F24H	0.1	1.2
F24A	0.0	0.1
F24H, L40R, T59D_M61S	0.0	0.0
F24H, L40R, T59N_M61S	0.1	1.1
F24H, L40R, T59S_M61S	0.0	0.0
F24H, R356K	0.1	0.3
F24H, T59R	0.0	0.0
F24H,T59N	0.0	0.0
F24W	0.0	0.0
F24Y	0.6	0.9
F24Y, L40R	0.0	0.0
F24Y, L40R, T59N	0.0	0.2
F24Y,R305K	0.0	0.2
F24Y,T59N	0.0	0.2
F24Y,T59N,R305K	0.0	0.1
F60W	0.2	0.5
G79A	0.0	-0.5
I83T	0.0	0.0
I83V	0.0	0.0
L40A	0.2	0.4
L40R	1.2	1.5
L40S	0.2	0.6
L40W	0.8	1.2
M61H	0.0	0.0
M61N	0.0	0.0
M61S	0.3	0.5
N23K	0.8	0.8
N23Q	0.2	0.6
S143K	0.6	0.4
S22I, T59A	0.0	-0.1
S22Q, T59Q	0.0	0.1
S57H, M61H	0.0	0.0
T18L, T59Q, M61N, F452W	0.0	0.0
T18S_T20S	0.6	1.2

T20A	0.0	0.0
T20C	0.1	0.1
T20S	0.6	1.4
T20S, L40D	0.0	0.0
T20S, L40E	0.2	0.6
T20S, L40F	0.2	0.3
T20S, L40H	0.0	0.0
T20S, L40K	0.0	0.0
T20S, L40Q	0.1	0.5
T20S, L40R	0.0	0.0
T20S, L40R, F60E	0.0	0.0
T20S, L40R, F60Q	0.0	0.0
T20S, L40R, N81E	0.0	0.0
T20S, L40R, N81Q	0.4	0.3
T20S, L40R, T59K	0.0	0.0
T20S, L40R, T59K_M61S	0.0	0.0
T20S, T59Q, M61T	0.0	-0.1
T20S,M61A	0.0	0.0
T20S,M61C	0.1	0.2
T20S,M61D	0.0	0.0
T20S,M61G	0.0	0.0
T20S,M61L	0.0	0.0
T20S,M61N	0.0	0.0
T20S,M61S	0.0	0.1
T20S,M61T	0.0	0.4
T20S,M61V	0.0	0.0
T20S,T59N	0.0	0.1
T20S,T59S_M61S	0.3	0.7
T20S_F24H	0.0	0.1
T20S_F24Y	0.0	0.2
T20S_F24Y,T59N	0.0	0.0
T2A	0.0	0.0
T2C	0.0	0.0
T2S	0.0	0.3
T2S,T18S_T20S	0.1	0.3
T2S,T18S_T20S,T59S_M61S	0.0	0.0
T2S,T20S	0.1	0.1
T2V	0.0	0.0
T59H_M61A	0.0	0.0
T59H_M61T	0.0	0.0
T59M	0.0	0.0
T59N	0.2	0.9
T59Q	0.0	0.0
T59Q, M61Q, F452W	0.0	0.0

T59S, M61H	0.0	0.1

Supplemental Figure S1

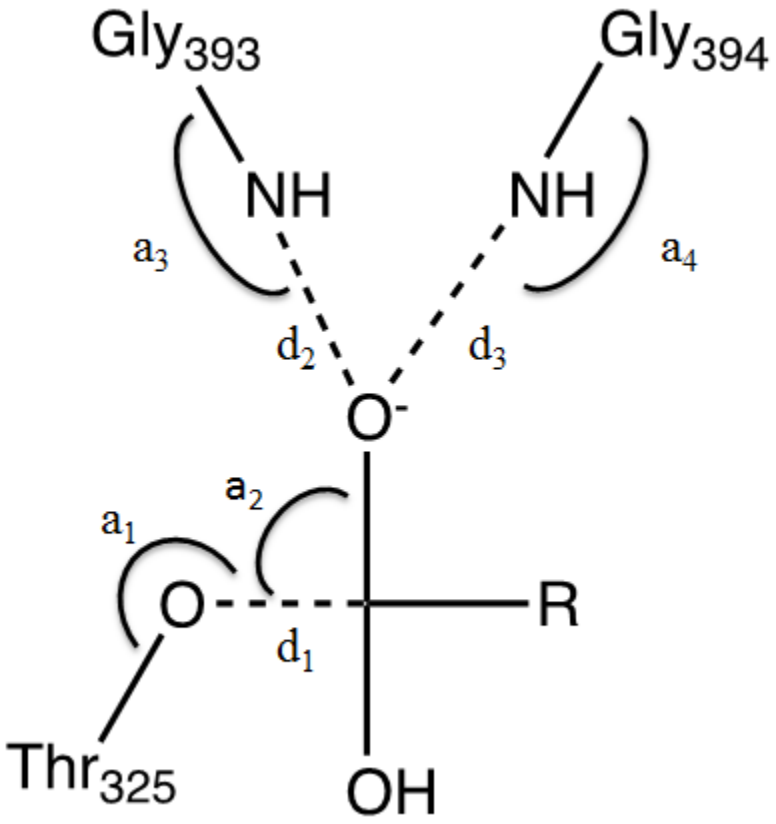

d_1	1.5 ± 0.1
d_2	2.8 ± 0.1
d_3	2.8 ± 0.1
a_1	109 ± 5
a_2	109 ± 5
a_3	120 ± 5
a_4	120 ± 5

Supplemental Figure S2

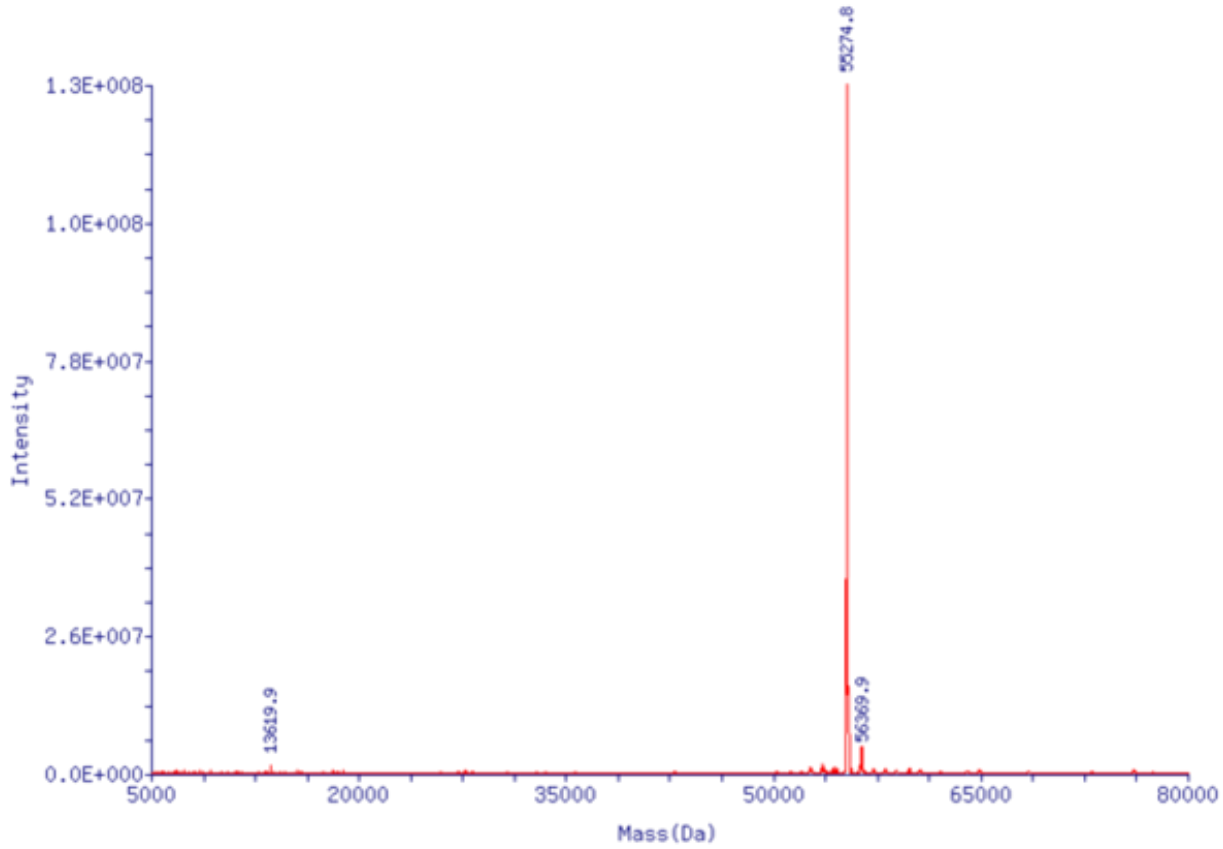

Supplemental Figure S3

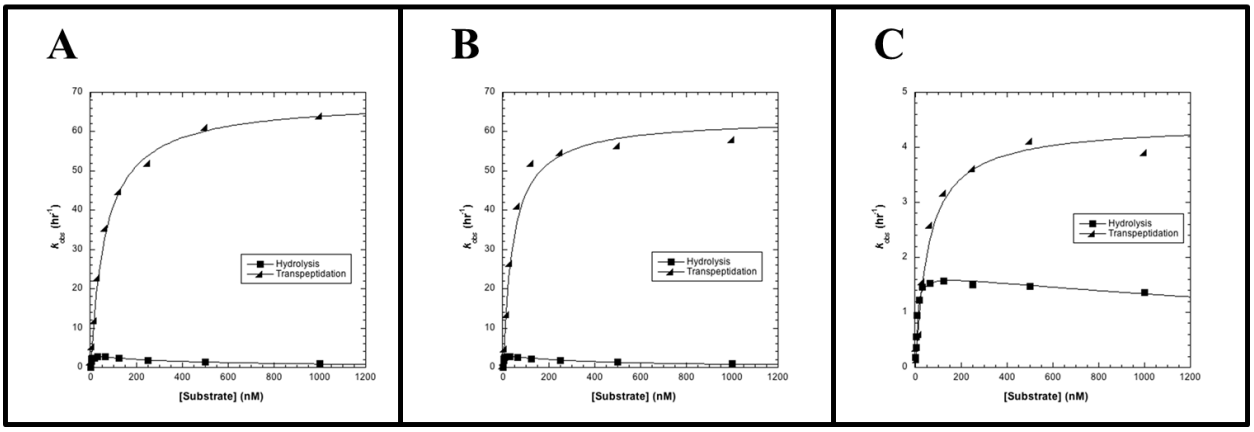

Supplemental Figure S4

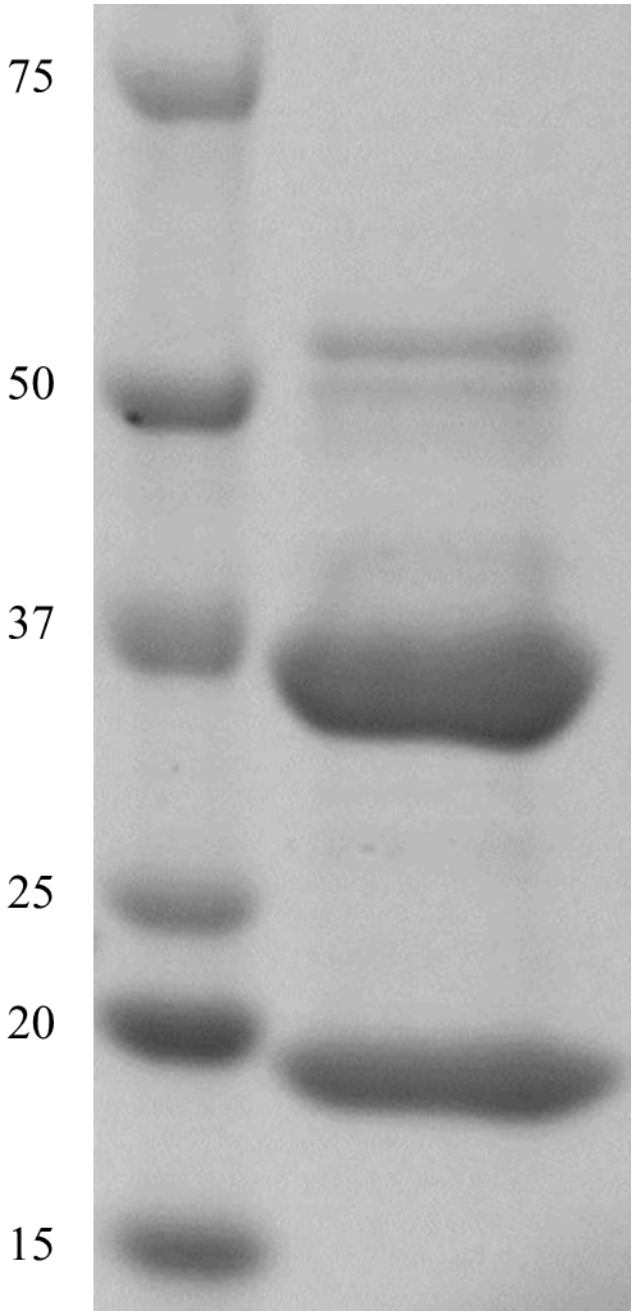

Supplemental Figure S5

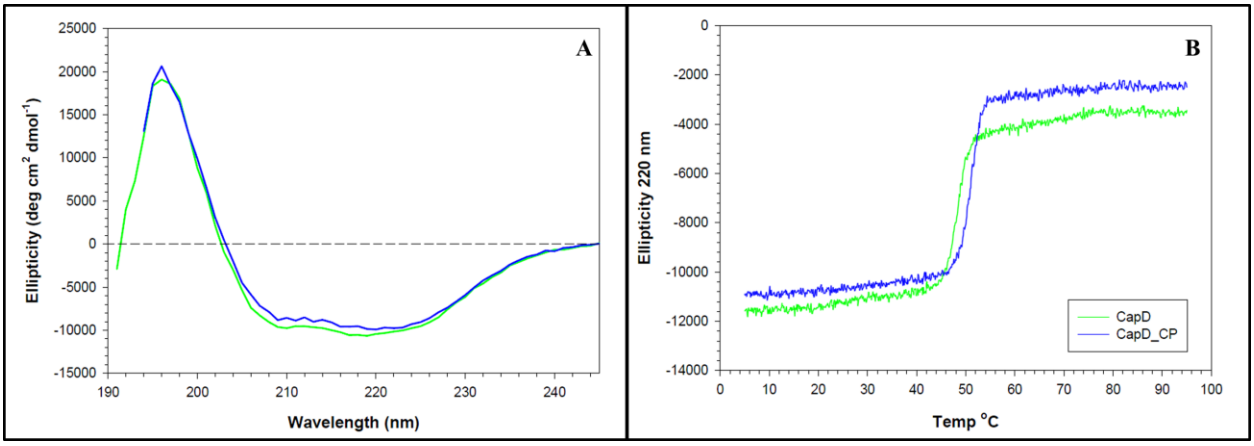

Supplemental Figure S6

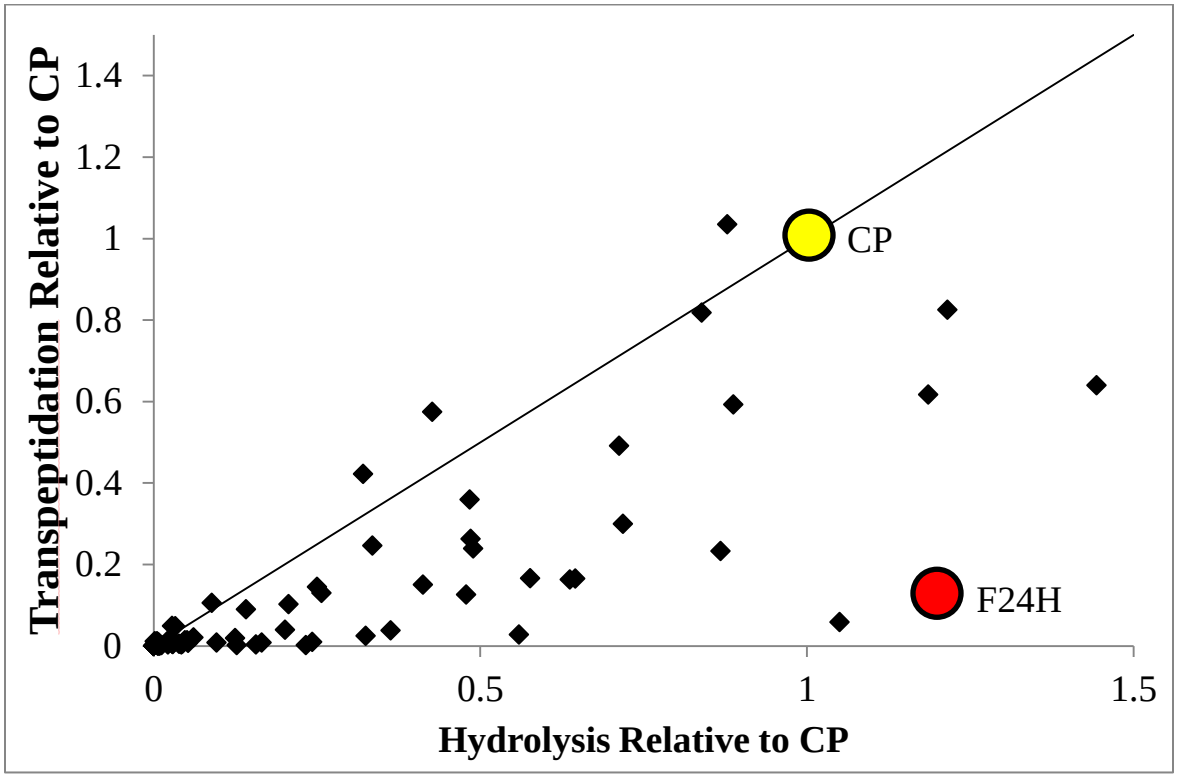

Supplemental Figure S7

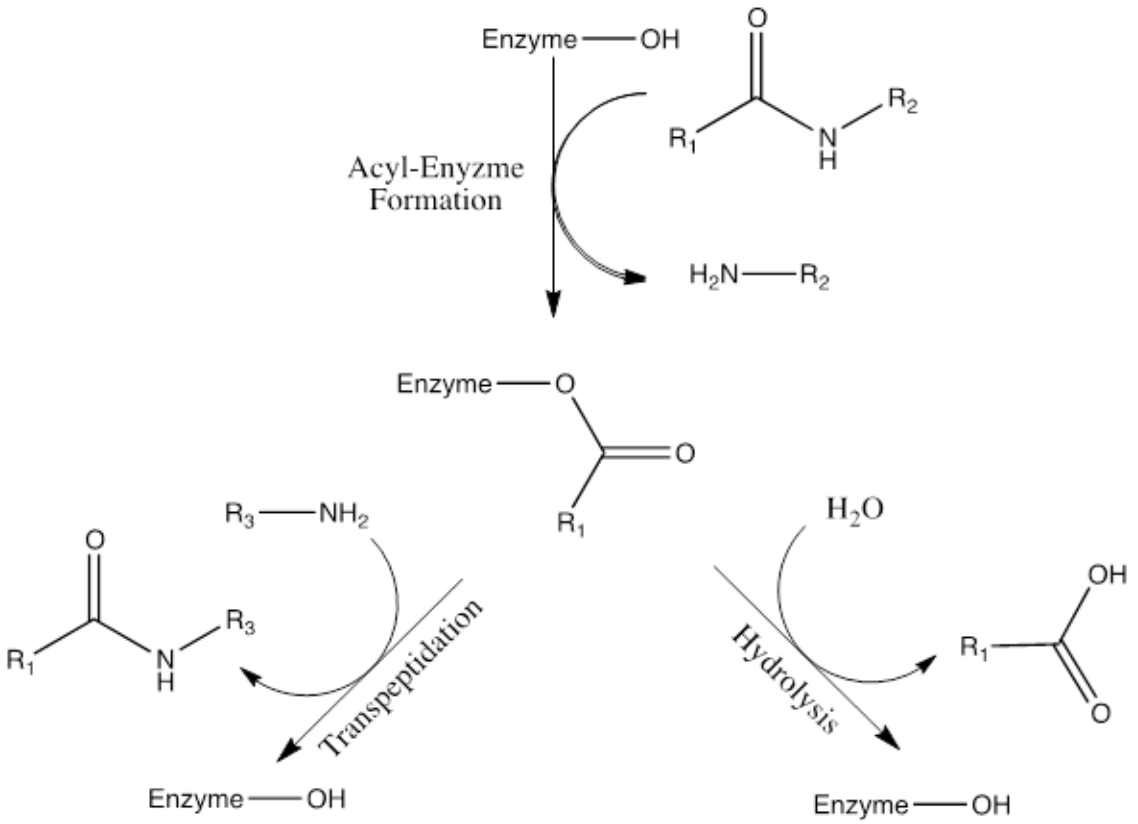

Supplemental Figure S8